International Journal of Advanced Scientific Research
www.allscientificjournal.com
ISSN: 2456-0421
Received: 20-12-2025, Accepted: 19-01-2026, Published: 03-02-2026
Volume 11, Issue 1, 2026, Page No. 62-71

Analysis and application of activated tamarind kernel powder for industrial wastewater treatment

Odimgbe E Izudike[1], Olubunmi A Adewusi[2], Apuyor S Ejohwomu[3], Clark D Poro[4], Adedeji A Olubunmi[5]
[1] Department of Industrial Chemistry, Ebonyi State University, Abakaliki, Nigeria
[2] Department of Chemistry, Lagos State University, Ojo, Lagos, Nigeria
[3] Department of Industrial Chemistry, Dennis Osadebay University, Asaba, Delta, Nigeria State
[4] Department of Chemistry, Federal University of Petroleum Resources, Effurun, Nigeria
[5] Department of Chemical Science, Lead City University, Ibadan, Oyo State, Nigeria

Abstract
Activated tamarind kernel powder was prepared from tamarind seed (Tamarindus indica); and utilized for the removal of Acid Red 1, Reactive Orange 20 and Reactive blue 29 dyes from their aqueous solutions. The powder was activated using 4M nitric acid (HNO_3). The effect of various parameters which include; pH, adsorbent dosage, ion concentration, and contact time were studied to identify the adsorption capacity of the activated tamarind kernel powder under the above conditions. The percentage of dye adsorbed is seen to be dependent on these factors. The result obtained indicated that the adsorption of Acid Red 1 (AR1), Reactive Orange 20 (RO20) and Reactive Blue 29 (RB29) decreased with increase in initial concentration but increased with increase in temperature. At equilibrium, all three dyes showed highest dye uptake at initial dye concentration of 20 mg/l, pH 2, adsorbent dose of 1.0 g, and at a contact time range of 80-100 min. The Temkin isotherm model is best-fitted into the experimental data with R^2 values ranging between 0.913-0.987 for Acid Red 1, 0.865-0.969 for Reactive Orange 20 and 0.942-0.992 for Reactive Blue 29. The next in line for best fitting is the Langmuir isotherm with R^2 values ranging between 0.859-0.995 for Acid Red 1 dye, 0.825-0.974 for Reactive Orange 20 and 0.971-0.989 for Reactive Blue 29. This is followed by Dubinin Radushkevich isotherm with R^2 values ranging between 0.931-0.974 for Acid Red 1, 0.923-0.989 for Reactive Orange 20 and 0.789-0.923 for Reactive Blue 29. Lastly is the Freundlich isotherm with R^2 values ranging between 0.803-0.931 for Acid Red 1, 0.856-0.964 for Reactive Orange 20 and 0.982-0.995 for Reactive Blue 29. Characterization of the activated tamarind kernel powder which was carried out using standard methods, showed that the values of the parameters of interest such as moisture and dry matter content, ash content, pH and bulk density; fall within acceptable range. Therefore, activated tamarind kernel powder has proven to be a very good adsorbent for the removal of acid dyes and reactive dyes.

Keywords: Tamarind kernel powder, industrial wastewater, treatment

Introduction

Water is the lifeblood of ecosystems, human societies, and industrial processes. Clean and accessible water is fundamental to maintaining life, health, and biodiversity (Obruche *et al*., 2025) [12]. However, the rapid pace of industrialization and urbanization has contributed to the contamination of natural water resources, creating a major environmental concern. Industrial activities, such as manufacturing, chemical processing, mining, and agriculture, release large volumes of wastewater containing harmful pollutants, including heavy metals, organic compounds, dyes, oils, and various chemicals (Al-Degs *et al*., 2004) [2]. The discharge of untreated or inadequately treated industrial effluents into natural water bodies poses a significant threat to both human health and the environment (Umudi *et al*., 2025) [22]. Contaminated water can lead to the spread of waterborne diseases, disruption of aquatic ecosystems, and degradation of biodiversity, all of which underscore the importance of effective wastewater treatment solutions (Itodo *et al*., 2021) [11]. As the global population continues to grow, so does the demand for clean water and the challenge of treating wastewater (Andre *et al*., 2011) [3]. Traditional wastewater treatment methods, such as chemical coagulation, membrane filtration, and activated carbon adsorption, have been widely used to mitigate the impacts of industrial effluents (Obruche *et al*., 2019) [14]. However, these conventional techniques often have limitations, including high operational costs, the production of secondary pollutants (e.g., sludge), and energy-intensive processes. Moreover, the complex nature of industrial wastewater, which often contains a wide variety of pollutants, makes it difficult to treat using a one-size-fits-all approach. Therefore, there is an increasing need for alternative, cost-effective, and environmentally sustainable materials and methods to treat industrial wastewater effectively (Ekpo *et al*., 2023) [21]. Industrial wastewater is a diverse and complex mix of pollutants, including toxic metals like lead, mercury, cadmium, and chromium, as well as organic compounds such as dyes, phenols, oils, surfactants, and solvents. These contaminants can have adverse effects on aquatic life and human health. Heavy metals, for example, can accumulate in the food chain, leading to poisoning and long-term health issues such as neurological damage, kidney failure, and cancer. Similarly, organic dyes used in industries such as textiles and pharmaceuticals can cause color pollution and inhibit light penetration in water, harming aquatic organisms (Obruche *et al*., 2018) [16]. Other organic pollutants, like phenols and oils, can degrade water quality and disrupt the delicate balance of aquatic ecosystems. The removal of these pollutants from wastewater is a challenging task due to the variety and persistence of contaminants. Existing treatment methods, such as chemical precipitation, electrocoagulation, reverse osmosis, and activated carbon adsorption, are often

effective in certain applications but can be costly, energy-intensive, or generate secondary waste that requires further treatment (Arita *et al*., 1995; Umudi *et al*., 2025) [4, 24]. Given these challenges, researchers have turned to alternative, low-cost materials that can be used to remove pollutants from wastewater. The use of natural materials for wastewater treatment has gained increasing attention due to their environmental benefits, availability, and low cost. These materials, often derived from agricultural by-products, have the potential to replace or complement traditional treatment methods. Agricultural by-products such as rice husks, coconut shells, and tamarind seeds are abundant, biodegradable, and can be chemically modified to enhance their adsorption capabilities. Moreover, using agricultural waste for wastewater treatment offers the added benefit of reducing waste disposal problems and providing a sustainable alternative to synthetic adsorbents. One such material that has shown promise for wastewater treatment is tamarind kernel powder (TKP). Tamarind (Tamarindus indica) is a tropical tree native to Africa and widely cultivated in Asia and other parts of the world. Tamarind kernel powder (TKP) has attracted interest for its ability to adsorb various pollutants from water, thanks to its chemical composition and physical characteristics (Bapat *et al*., 2006) [6]. The presence of hydroxyl, carboxyl, and amino groups on the surface of tamarind kernel powder makes it highly reactive and capable of interacting with a wide range of pollutants. These functional groups facilitate the binding of pollutants such as metal ions, organic dyes, and other toxic compounds, making TKP an effective biosorbent for wastewater treatment. The high surface area and porosity of tamarind kernel powder also contribute to its adsorption capacity. When treated, tamarind kernel powder can act as a filter to capture contaminants from wastewater. Activation is the process of modifying the physical and chemical properties of a material to increase its adsorption capacity. Tamarind kernel powder, in its natural form, can be activated through chemical or physical methods (El-Hendawy *et al*., 2008) [8]. The activation of tamarind kernel powder significantly improves its effectiveness in removing pollutants from wastewater. Activated tamarind kernel powder (ATKP) has been shown to exhibit enhanced adsorption capacities for heavy metals such as lead, cadmium, and chromium, as well as for organic compounds like methylene blue dye. This makes it an attractive material for use in industrial waste treatment, where the removal of both organic and inorganic contaminant is often required (Erienu *et al*., 2022) [9].

The aim of this research is to investigate the effect of the tamarind kernel powder for industrial waste treatment.

Materials and Method

Materials

Sample Collection, Identification and Treatment

The procedure for sample collection, identification, and treatment adhered to the methodology established by Obruche *et al*. (2019) [18]. Tamarind kernel fruit was sourced from the local market in Samaru, located within the Sabongari Local Government Area of Kaduna State. Following collection, the samples were transported to the Biological Sciences Department at Ahmadu Bello University, where they were identified as Tamarindus indica. The Tamarind kernel seeds underwent thorough washing with water to eliminate any adhering materials. Subsequently, the reddish testa of the seeds was removed by heating them in an oven at 800 °C for duration of 2 hours. The kernels were then ground and placed in the oven at a temperature of 300 °C for 3 hours to ensure complete carbonization of the tamped powder. The resulting powder was sieved through a 400-micron mesh to achieve a uniform particle size suitable for use. The dye samples, Acid Red 1, Reactive Orange 20, and Reactive Blue 29, were procured from Sigma Aldrich Company.

Adsorbate Preparation

Stock solutions (1.0 g/L) of Acid Red 1, Reactive Blue 29, and Reactive Orange 20 were created by dissolving approximately 1 gram of each dye in 1 liter of distilled water. All test solutions with the desired concentrations were prepared through successive dilutions to achieve the required initial experimental concentration ranging from 20 to 100 mg/L.

Preparation of Activated Tamarind Kernel Powder

The method for sample preparation was based on the work of Umanah *et al*. (2025) [25], with minor modifications. The activated tamarind kernel powder was prepared following the procedure outlined by Shanthi and Mahalakshmi (2012). Approximately 200 grams of the sieved carbon was combined with 200 mL of 4M nitric acid. This mixture was then placed in an oven at 105 °C for 30 minutes, with occasional stirring, before being removed and allowed to sit overnight. After cooling, the activated tamarind kernel powder was washed repeatedly with double distilled water until the pH of the filtrate was between 6 and 6.5. The adsorbent was subsequently dried in an oven at 105 °C for 1 hour and stored in a desiccator.

Moisture and Dry Matter Content

The Moisture and Dry Matter Content were assessed following the methodology outlined by Festus-Amadi (2021) [10], Obruche *et al*. (2019) [18], and Abeokuta *et al*. (2025) [1], with certain modifications. Clean silica crucibles were dried in a desiccator and subsequently weighed. A precise amount of 1g of the dry tamarind kernel powder was measured as W1. This sample was then dried in an air-circulated oven at 105 °C for duration of 3 hours, after which it was cooled in a desiccator, and the final weight was recorded as W2.

Ash Content Determination

This determination was conducted in accordance with ASTM E1755-01. A copper crucible was subjected to heating in a furnace at 575 °C for four hours, then cooled in a desiccator and weighed. The sample that had been oven-dried from the moisture content analysis was utilized. The crucible containing the dry sample was placed in a muffle furnace, where the temperature was allowed to rise to 575 °C. After approximately 6 hours, it was removed, allowed to cool in a desiccator, and the weight was recorded as W3. It was then returned to the furnace at 575 °C for one hour until a consistent weight of ± 0.3g was achieved (ASTM, 2003) [5].

PH Measurements

The activated TKP sample was boiled in double distilled water utilizing a reflux condenser to recycle the water vapor. The TKP particles were filtered out; subsequently, the filtrate was cooled to 50°C, and the pH of the filtrate

was measured using electrometric methods (ASTM, 2003) [5].

Bulk Density

The displacement method was employed for this analysis (Umudi *et al*., 2025) [24]. This involved measuring the volume of double distilled water displaced when a known weight (2g) of the sample was introduced into 50 ml of double distilled water contained within a 100 ml graduated measuring cylinder.

Adsorption Experiment

Effect of Initial Dye Concentration

The adsorption experiment was conducted using a batch method (Oladunni *et al*.; 2012) [15]. The experiment was performed at ambient temperature (298 K) utilizing a basic reciprocating shaker, with a 120 ml glass bottle serving as the reactor. The working initial dye concentrations were set at 20, 40, 60, 80, and 100 mg/L.

Effect of Adsorbent Dose

The impact of adsorbent dosage was assessed at a steady pH of 6, an initial dye concentration of 20 mg/L, and a stirring duration of 2 hours. The adsorbent dosage was adjusted to 0.4, 0.6, 0.8, 1.0, and 1.2 g.

Effect of Initial pH

The influence of initial pH was evaluated by changing the pH while keeping the temperature constant at 298 K, adsorbent dosage at 0.2 g, initial concentration at 20 mg/L, and agitation time at 2 hours. The pH levels were modified to 2, 4, 6, 8, and 10 using 0.1M HCl and 0.1M NaOH to raise or lower the pH of the solution.

Effect of Contact Time

The effect of contact time is crucial in adsorption research as it aids in understanding the kinetics of adsorption. The contact time was analyzed by stirring the mixture at different time intervals. The stirring was done at a constant temperature of 298 K, with an adsorbent dosage of 0.2 g, an initial concentration of 20 mg/L, and a pH of 6. The contact times were set at 20, 40, 60, 80, and 100 minutes.

Effect of Temperature

The effect of temperature is significant for this research as it provides essential data for the adsorption thermodynamic study. This was determined by stirring the mixture at various temperatures and initial dye concentrations. The stirring was conducted at a constant adsorbent dosage of 0.2 g, a pH of 6, and a contact time of 2 hours. The temperatures used were 298, 308, 318, 323, and 328 K.

Adsorption Isotherms

The adsorption isotherms utilized in this study are detailed in chapter 2.4.5. The Langmuir adsorption isotherm was derived by plotting Ce/qe against Ce, with the Langmuir constant KL and qm being determined from the intercept and slope of the Langmuir plot, respectively. The Freundlich adsorption isotherm was established by plotting logqe against logCe, where Kf and n are the Freundlich constants obtained from the intercepts and slopes of the Freundlich plot. The Temkin isotherm was derived from a linear plot of qe versus lnCe, with the Temkin constant bT and the equilibrium binding constant AT being obtained from the intercepts and slopes of the Temkin plot. The Dubinin-Radushkevich isotherm was established by plotting ln qe against ε2, with values of qs and B determined from the slope and intercepts of the D-R plot (Umudi *et al*., 2205) [28].

Adsorption Kinetics

The adsorption kinetics examined in this research are referenced from (Oladoja *et al*., 2008) [17]. The Pseudo first order plot was created by plotting log (qe-qt) against t, with the value of k1 derived from the slope of the graph, while the calculated qe was obtained from the graph's intercept. The Pseudo second order plot was generated by plotting t/qt against t, with 1/qe and 1/k q 2 serving as the slope and intercept, respectively.

Results and Discussion

Characterization of Activated Tamarind Kernel Powder

Moisture and Dry Matter Content of ATKP

The moisture content of activated TKP is recorded at 3.45% moisture and 96.55% dry matter. This moisture percentage is lower compared to the values reported for Khaya senegalensis fruit (6.17%), walnut shell (4.18%), Delonix regia (6.286%), and Locust bean husk (8.20%) as noted by Obruche *et al*., (2018). The low moisture and high dry matter content of the ATKP suggest that it is a highly effective material for adsorption processes.

Bulk Density of TKP

The bulk density of activated tamarind kernel powder, as shown in Table 1, was determined to be 0.4 g/cm3. This value exhibited some discrepancies when compared to the findings of Oladunni *et al*. (2012), who reported a density of 0.49 g/cm3 for locust bean husk, and 0.26 g/cm3 for other materials. Furthermore, Oladunni *et al*. (2012) [15] indicated that a higher bulk density in an adsorbent correlates with increased volume activity, which serves as a marker of superior adsorbent quality.

Ash Content of ATKP

The ash content percentage of the activated tamarind kernel powder, detailed in Table 1, was measured at 5.30%. This relatively low ash content suggests that the ATKP possesses minimal inorganic material and a significant amount of fixed carbon. In comparison, Ekpo *et al*. (2025) [7] reported an ash content of 2.14% for almond shells.

pH of ATKP

The pH level of the activated tamarind kernel powder was recorded at 6.45, as illustrated in Table 1, which falls within the acceptable range for an optimal adsorbent. Olugbenga *et al*. (2010) [20] noted a pH of 6.30 for rice husk carbon.

Table 1: Physicochemical Parameters of Tamarind Kernel Powder

Parameters	TKP
Dry matter content (%)	96.55
Moisture content (%)	3.45
pH	6.40
Bulk Density ($g.cm^{-3}$)	0.40
Ash content (%)	5.30

FTIR Analysis of ATKP

A Fourier Transform Infrared Spectroscopy (FTIR) analysis was conducted to examine and identify the functional

groups present in the adsorbents within the range of 650 cm-1 to 4000 cm-1. The spectra illustrating the functional groups and their corresponding peaks for both the activated tamarind kernel powder and the dye-treated activated tamarind kernel powder are displayed in Figures 1 – 4. The findings indicate the presence of various functional groups, including Phosphates (P-O-C), alkenyl (-C=C-Stretch), conjugated (-C=C-Stretch), alkanes (C-H stretch), alkenes (=C-H stretch), alkynes (-C≡C-), carboxylic acids (O-H bend), aromatic amines (C-N), nitrites (C≡N stretch), aromatics (C-H stretch), alkyl halides, and primary alcohols (C-O Stretch), among others. A notable shift in the wave number of the prominent peaks associated with the spectra suggests the diverse activities of functional groups on the activated tamarind kernel powder. These activities have been characterized by the interactions between the functional groups on the adsorbent's surface and those present in the dye molecule. Specifically, a shift from 3261.4 cm^{-1} in the ATKP spectrum (O-H stretch, carboxylic acid) to 3257.7 cm^{-1} in the RB29 spectrum indicates an O-H (broad) stretch of a hydrogen-bonded hydroxyl group, while a peak at 3343.4 cm^{-1} in the RO20 spectrum signifies an O-H stretch of a hydrogen-bonded hydroxyl group. A transition from 2922.2 cm-1 observed in the ATKP and RO20 spectra (figure 3),
which signifies the H-C-H stretching in alkanes, to 2926.4 cm^{-1} in the AR1 (figure 2) and RB29 spectra (figure 4), indicating the methyl C-H asymmetric/symmetric stretching. Furthermore, a shift from 2109.7 cm^{-1} in the ATKP and RB29 spectra (figure 4), which denotes the -C≡C- stretching in alkynes, to 2113.4 cm^{-1} in the AR1 and RO20 spectra, also indicates the methyl C-H asymmetric/symmetric stretching. Additionally, a transition from 1699.7 cm^{-1} in the ATKP and AR1 spectra (figure 2), which suggests the presence of -C=C- stretching in alkenes, to 1703.4 cm^{-1} in the RB29 and RO20 spectra, indicates the presence of aromatic combination bands. Moreover, a shift from 1606.5 cm^{-1} in the ATKP, AR1 (figure 2), and RB29 spectra (figure 4), which indicates the presence of an aromatic ring stretch, quinone or conjugated ketone, open chain azo, primary amine NH bend, or secondary amine NH bend, to 1617.7 cm^{-1} in the RO20 spectrum, indicates the presence of an open chain azo. Lastly, a transition from 1237.5 cm-1 in the ATKP spectrum, indicating the presence of C-N stretching in aromatic amines, to 1241.2 cm^{-1} in the ARI (figure 2), RB29 (figure 4), and RO20 spectra (figure 3), indicates the presence of aromatic ethers, Aryl-O stretching, or aromatic phosphates (P-O-C stretching). The presence of hydroxyl groups, carbonyl groups, ethers, and aromatic compounds serves as evidence of the lingo-cellulosic structure of tamarind kernel powder, which has also been observed in other materials such as coconut shell (Ucello-Berrata *et al*., 2008).

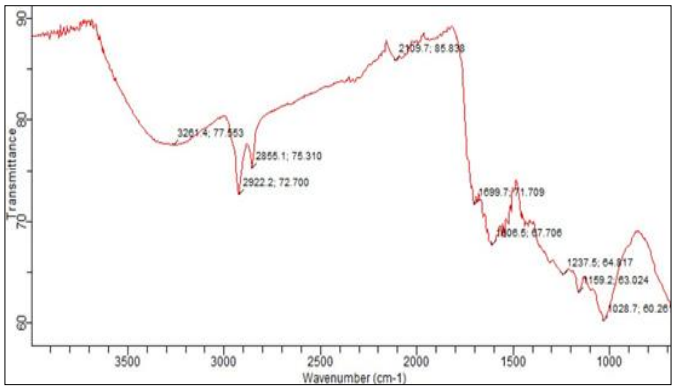

Fig 1: FTIR Spectrum of Activated Tamarind Kernel Powder

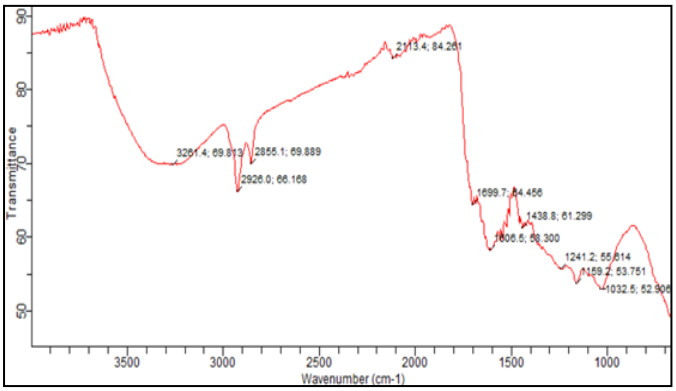

Fig 2: FTIR Spectrum of Acid Red 1 Treated TKP

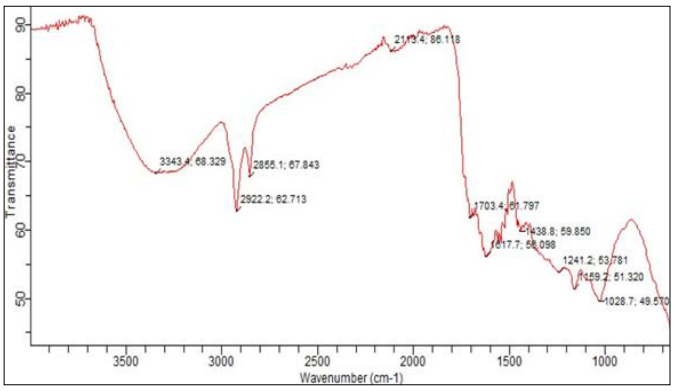

Fig 3: FTIR Spectrum of Reactive Orange 20 Treated TKP

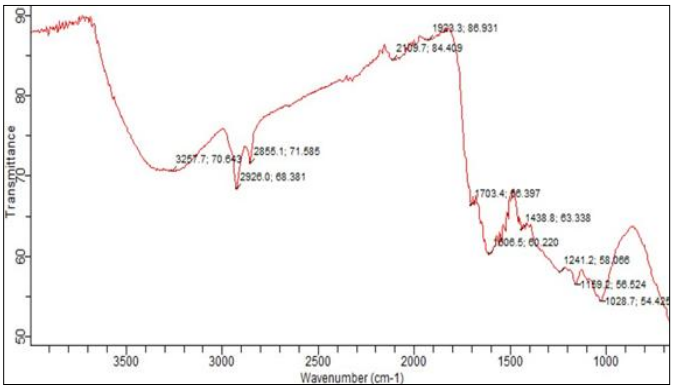

Fig 4: FTIR Spectrum of Reactive Blue 29 Treated TKP

Adsorption Studies

Effect of pH on the Adsorption Process

The pH level influences the extent of ionization and speciation of the adsorbate, specifically the dye solutions in this context, and is therefore considered a crucial factor in adsorption research. The percentages of dye adsorption, as illustrated in Table 2, ranged from 95.00% to 61.00% for Acid Red 1 dye, 80.00% to 9.00% for Reactive Orange 20 dye, and 85.00% to 20.00% for Reactive Blue 29 dye. The findings indicated that the percentage of AR1, RO20, and RB29 dyes adsorbed diminished as the pH value increased for all three dyes. This suggests that a lower pH is

advantageous for the adsorption of AR1, RO20, and RB29 by the adsorbent, attributable to the anionic characteristics of these dyes. This phenomenon arises from an increase in the number of positively charged sites, which occurs due to a reduction in negatively charged sites as the pH of the system decreases. Consequently, this enhances the adsorption of the negatively charged dye anions through electrostatic attraction. Comparable results were documented by Okoli *et al*. (2015) [13] and Ogwuche & Obruche (2020) [19].

Table 2: Effect of Initial pH on Dye Adsorption onto TKP

Acid Red 1			Reactive Orange 20		Reactive Blue 29	
pH	q_e (mg/l)	R (%)	q_e (mg/l)	R (%)	q_e (mg/l)	R (%)
2	4.75	95.0	4.00	80.0	4.25	85.0
4	4.15	83.0	4.93	30.0	2.55	51.0
6	3.85	77.0	1.05	21.0	2.00	40.0
8	3.50	70.0	0.75	15.0	1.23	24.5
10	3.05	61.0	0.45	9.0	1.00	20.0

Effect of Adsorbent Dosage on the Adsorption Process

The findings derived from this experiment demonstrated that with an increase in adsorbent dosage (ranging from 0.4g to 1.2g), the percentage of dye adsorption also rose, specifically from 65.0% to 86.5% for AR1, from 40.0% to 64.0% for RO20, and from 40.0% to 54.0% for RB29, as illustrated in table 3. The adsorption percentage continued to rise until reaching 1.0g of adsorbent, beyond which there were no notable changes in the percentages of dye adsorbed despite further increases in the adsorbent quantity. This observation corroborated the findings of Okoli *et al*. (2015) [13], who noted that "most of the adsorbents examined reached equilibrium at approximately 1.0g of dosage, and any additional increase in the adsorbent amount led to a decrease in the quantity of dye removed from the solution.

Table 3: Effect of Adsorbent Dose (A.D.) on Dye Adsorption onto TKP

Acid Red 1			Reactive Orange 20		Reactive Blue 29	
A.D. (g)	q_e (mg/l)	R (%)	q_e (mg/l)	R (%)	q_e (mg/l)	R (%)
0.4	1.63	65.0	1.00	40.0	1.00	40.0
0.6	1.21	72.5	0.73	43.5	0.73	44.0
0.8	1.00	80.0	0.69	55.0	0.62	49.5
1.0	0.86	86.0	0.63	62.5	0.54	53.5
1.2	0.70	85.0	0.50	60.0	0.43	52.0

Effect of Contact

The influence of batch contact time on the percentage of dye removal was examined. It was noted that the percentage of dye removal increases significantly with an initial rise in contact time, and subsequently, after approximately 80 minutes of contact time, no significant change in the percentage removal was detected. When the contact time was extended from 20 minutes to 100 minutes, the percentage of dye removal increased from 62.5% to 79.0% for AR1, from 20.0% to 30.0% for RO20, and from 37.5% to 51.5% for RB29, as illustrated in Table 4. Consequently, the optimal contact time is identified as 80 minutes. This duration is also regarded as the equilibrium time for the batch adsorption experiment, since beyond 80 minutes, the rate of adsorption remains unchanged. The results indicate a rapid dye removal at the onset of contact time, attributed to the abundance of binding sites available for adsorption and the initial concentration gradients between the adsorbate in solution and the vacant sites on the TKP surface at the start. The gradual increase in adsorption and the subsequent achievement of equilibrium may be linked to the limited mass transfer of molecules from the bulk liquid to the external surface of the adsorbent. During this phase, adsorption predominantly occurred on the adsorbent's surface. Moreover, the reduced removal rate is a consequence of the saturation of binding sites by dye molecules, as reported by Ugochukwu *et al*. (2025) [27].

Table 4: Effect of Contact Time on Dye Adsorption onto TKP

Acid Red 1			Reactive Orange 20		Reactive Blue 29	
Time (min)	q_e (mg/l)	R (%)	q_e (mg/l)	R (%)	q_e (mg/l)	R (%)
20	3.1	62.5	1.0	20.0	1.9	37.5
40	3.5	70.0	1.08	21.5	2.1	41.0
60	3.8	75.0	1.3	25.0	2.4	47.5
80	4.0	80.0	1.5	30.0	2.6	51.5
100	4.0	80.0	1.5	30.0	2.6	51.5

Effect of Initial Dye Concentration

The adsorption of ARI, RO20, and RB29 dyes was examined using initial concentrations of 20, 40, 60, 80, and 100 mg/l for each of AR1, RO20, and RB29, while maintaining a constant adsorbent dose and pH across various operating temperatures. The initial concentration of the adsorbate is crucial, as a specific mass of adsorbent can only adsorb a limited quantity of solute. As shown in Table 5, the percentage removal of the dyes decreased with an increase in the initial dye concentration, specifically from 76.0% to 54.0% for Acid Red 1, from 31.0% to 20.0% for Reactive Orange 20, and from 51.5% to 38.0% for Reactive Blue 29. These results suggest that as the concentration of the solution increases, the proportion of dye that a given mass of adsorbent can effectively adsorb diminishes. In lower concentration ranges, the fractional adsorption is significantly higher compared to that in higher concentration ranges. This phenomenon can be attributed to the greater availability of adsorption sites at lower concentrations, whereas at elevated concentrations, the number of available sites decreases. At lower concentrations, the adsorption sites can quickly capture the available dye molecules, while at higher concentrations, the dye molecules must diffuse to the adsorbent surface through intra-particle diffusion. Consequently, the percentage of dye removal is influenced by the initial concentration. Similar observations have been documented by Obruche *et al*. (2025) [12].

Table 5: Effect of Initial Concentration on Dye Adsorption onto TKP

Acid Red 1			Reactive Orange 20		Reactive Blue 29	
C_o (mg/l)	q_e (mg/l)	R (%)	q_e (mg/l)	R (%)	q_e (mg/l)	R (%)
20	3.8	76.0	1.6	31.0	2.6	51.5
40	7.8	78.3	2.8	28.0	4.8	48.0
60	10.0	66.7	4.1	27.0	6.8	45.0
80	11.8	58.8	5.0	25.0	8.0	40.0
100	13.5	54.0	5.0	20.0	9.5	38.0

Adsorption Isotherm Modelling

The adsorption isotherm data revealed that the amount of dye adsorbed increased with increasing equilibrium concentration of dyes. In this work, Freundlich, Langmuir, Temkin and Dubinin- Radushkevich isotherm were evaluated.

Langmuir Isotherm

The Langmuir isotherm represents the monolayer coverage of an adsorbate on the surface of an adsorbent at a constant temperature. The fundamental premise is that the forces exerted by chemically unsaturated surface atoms do not extend beyond the diameter of a single adsorbed molecule. This isotherm suggests a homogeneous surface. Table 6 illustrates the Langmuir adsorption isotherm models for Acid Red 1 across a temperature range of 298K to 328K. From Table 6, it is evident that the plots are linear, and the correlation coefficient (R2) values were determined to be 0.859, 0.917, 0.978, 0.991, and 0.995 at temperatures of 298K, 308K, 318K, 323K, and 328K, respectively, indicating adherence to the Langmuir isotherm model. The maximum adsorbate uptake (qm) for Acid Red 1 was recorded as 20.8 (mg/g), 18.87 (mg/g), 17.86 (mg/g), 17.24 (mg/g), and 16.67 (mg/g) at the respective temperatures of 298K, 308K, 318K, 323K, and 328K. The results indicate that qm, which also represents the number of available adsorption sites, decreases as the temperature rises from 298K to 328K. The constant b, which relates to the affinity coefficient of Acid Red 1 to activated tamarind kernel powder, was found to be 0.04 (l/mg), 0.06 (l/mg), 0.09 (l/mg), 0.13 (l/mg), and 0.18 (l/mg) at 298K, 308K, 318K, 323K, and 328K, respectively. The same Table 6 also presents the Langmuir adsorption isotherm models for Reactive Orange 20 within the temperature range of 298K to 328K. From Table 6, it can be observed that the values are linear, with correlation coefficient (R2) values of 0.907, 0.825, 0.930, 0.901, and 0.975 at 298K, 308K, 318K, 323K, and 328K, respectively, further confirming compliance with the Langmuir isotherm model. The maximum adsorbate uptake (qm) for Reactive Orange 20 was found to be 10.10 (mg/g), 9.01 (mg/g), 9.35 (mg/g), 9.61 (mg/g), and 8.54 (mg/g) at the respective temperatures of 298K, 308K, 318K, 323K, and 328K. The findings indicate that the maximum adsorbate uptake (qm) diminished as the temperature rose from 298K to 328K. The constant b, which pertains to the affinity coefficient of Acid Red 1 for activated tamarind kernel powder at temperatures of 298K, 308K, 318K, 323K, and 328K, is recorded as 0.04 (l/mg), 0.06 (l/mg), 0.09 (l/mg), 0.13 (l/mg), and 0.18 (l/mg) respectively. Table 6 illustrates the Langmuir adsorption isotherm models for Reactive Blue 29 across the temperature spectrum of 298K to 328K. As shown in Table 6, the values exhibit linearity, with correlation coefficients (R2) of 0.986, 0.989, 0.971, 0.983, and 0.977 at 298K, 308K, 318K, 323K, and 328K respectively, suggesting that the data aligns with the Langmuir isotherm model. The maximum adsorbate uptake (qm) for Reactive Blue 29 was determined to be 16.67 (mg/g), 16.67 (mg/g), 13.16 (mg/g), 12.82 (mg/g), and 12.98 (mg/g) at 298K, 308K, 318K, 323K, and 328K respectively. The results indicate a decrease in qm as the temperature increased from 298K to 328K. The constant b, which relates to the affinity coefficient of Reactive Blue 29 for activated tamarind kernel powder at 298K, 308K, 318K, 323K, and 328K, is noted as 0.02 (l/mg), 0.02 (l/mg), 0.06 (l/mg), 0.07 (l/mg), and 0.07 (l/mg) respectively. The observed reduction in maximum adsorbate uptake (qm) may be attributed to a rise in the number of dye molecules transitioning from the dye solution to the adsorbent's surface at elevated temperatures. The b values were observed to increase with rising temperatures, potentially due to enhanced activity of the dye molecules as they gain kinetic energy. The RL values derived from this investigation ranged from 0.05 to 0.35 for Acid Red 1 dye, 0.125 to 0.45 for Reactive Orange 20 dye, and 0.11 to 0.42 for Reactive Blue 29. Meanwhile, the correlation coefficients (R2) varied from 0.825 to 0.995 for Acid Red 1 dye, 0.859 to 0.974 for Reactive Orange 20 dye, and 0.971 to 0.989 for Reactive Blue 29, as the temperature increased from 298K to 328K. The results obtained from separation factor (RL) calculation showed that adsorption of Acid Red 1, Reactive Orange 20 and Reactive Blue 29 are favourable on activated tamarind kernel powder. Similar results are reported by Okoli *et al*., (2015) [13]

Table 6: Langmuir isotherm constants for AR1, RB29 and RO20

Tempt (K)	Dye	q_m(mg/g)	B(l/g)	R2	R_L
	Acid Red 1				
298		20.8	0.04	0.859	0.35
308		18.87	0.06	0.917	0.23
318		17.86	0.09	0.978	0.14
323		17.24	0.13	0.991	0.08
328		16.67	0.18	0.995	0.05
Reactive Blue 29					
298		16.67	0.02	0.986	0.42
308		16.67	0.02	0.989	0.36
318		13.16	0.06	0.971	0.18
323		12.82	0.07	0.983	0.13
328		12.98	0.07	0.977	0.11
Reactive Orange 20					
298		10.10	0.01	0.907	0.45
308		9.01	0.02	0.825	0.36
318		9.35	0.03	0.930	0.26
323		9.61	0.03	0.901	0.23
328		8.54	0.06	0.974	0.13

Freundlich Isotherm

The Freundlich isotherm represents an empirical equation utilized to characterize heterogeneous systems. It is widely regarded as a prominent model for single solute systems, predicated on the equilibrium distribution of solute between the solid and aqueous phases. The Freundlich constants, Kf and n, which correspond to the adsorption capacity of the adsorbent and the intensity of adsorption respectively, have been derived from the intercepts and slopes of the linear plot of lnqe versus lnCe, as illustrated in Table 7. The value of the adsorption intensity n serves as an indicator of the favorability of the adsorption process. The findings align with those reported by Okoli *et al*. (2015). Table 7 presents the Freundlich adsorption isotherm models for Acid Red 1 across a temperature range of 298K to 328K. The table reveals that the plots are linear, with correlation coefficient (R2) values of 0.803, 0.793, 0.863, 0.797, and 0.931 at temperatures of 298K, 308K, 318K, 323K, and 328K respectively, suggesting adherence to the Freundlich isotherm model. The adsorption capacity (Kf) of activated tamarind kernel powder for Acid Red 1 is recorded as 1.57 (l/g), 1.98 (l/g), 2.93 (l/g), 3.32 (l/g), and 3.97 (l/g) at the respective temperatures of 298K, 308K, 318K, 323K, and 328K. The results indicate that Kf, which denotes the adsorption capacity of the adsorbent, increases with rising temperature from 298K to 328K. The constant n, which pertains to the adsorption efficiency of activated tamarind kernel powder for Acid Red 1 at 298K, 308K, 318K, 323K, and 328K, is recorded as 1.73, 1.88, 2.12, 2.27, and 2.66 respectively. The same Table 7 also illustrates the Freundlich adsorption isotherm models for Reactive Orange 20 within the temperature range of 298K to 328K. The table

indicates that the values are linear, with correlation coefficient (R2) values of 0.964, 0.860, 0.915, 0.856, and 0.898 at 298K, 308K, 318K, 323K, and 328K respectively, further confirming adherence to the Freundlich isotherm model.The adsorption capacity (Kf) of activated tamarind kernel powder for Reactive Orange 20 was measured at 4.09 (l/g), 2.75 (l/g), 2.06 (l/g), 1.72 (l/g), and 1.00 (l/g) at temperatures of 298K, 308K, 318K, 323K, and 328K, respectively. The results indicate a decrease in Kf as the temperature rises from 298K to 328K. The constant n at these temperatures is recorded as 1.39, 1.51, 1.63, 1.68, and 2.12, respectively. Table 7 illustrates the Freundlich adsorption isotherm models for Reactive Blue 29 within the same temperature range of 298K to 328K. The table shows that the plots are linear, with correlation coefficient (R2) values of 0.982, 0.981, 0.989, 0.995, and 0.984 at 298K, 308K, 318K, 323K, and 328K, respectively, suggesting adherence to the Freundlich isotherm model. The adsorption capacity (Kf) for Reactive Blue 29 was found to be 1.71 (l/g), 1.36 (l/g), 1.72 (l/g), 2.05 (l/g), and 2.63 (l/g) at the same temperatures. The results demonstrate an increase in Kf as the temperature progresses from 298K to 328K. The constant n at these temperatures is 1.46, 1.55, 2.27, 2.46, and 2.90, respectively. The value of the adsorption intensity n provides insight into the favorability of the adsorption process, particularly when n is within the range of 1-10 (Ho and Chang, 2001). The Freundlich adsorption isotherm serves as a valuable tool for predicting the adsorption capacity of activated tamarind kernel powder for Acid Red 1, Reactive Orange 20, and Reactive Blue 29. A steeper isotherm indicates a more effective adsorbent (Umudi *et al*., 2025) [26].

Table 7: Freundlich Isotherm constants for AR1, RB29 and RO20

Tempt (K)	Dye	K_f(l/g)	N	R2
	Acid Red 1			
298		1.57	1.72	0.803
308		1.98	1.88	0.793
318		2.93	2.12	0.863
323		3.32	2.27	0.797
328		3.97	2.66	0.931
Reactive Orange 20				
298		4.09	1.39	0.964
308		2.75	1.51	0.860
318		2.06	1.63	0.915
323		1.72	1.68	0.856
328		1.00	2.12	0.898
Reactive Blue 29				
298		1.71	1.46	0.982
308		1.36	1.55	0.981
318		1.72	2.27	0.989
323		2.05	2.46	0.995
328		2.63	2.90	0.984

Temkin Isotherm

Table 8 illustrates the Temkin adsorption isotherm models for Acid Red 1 across a temperature range of 298K to 328K. As shown in Table 8, the values exhibit linearity, with correlation coefficient (R2) values recorded at 0.803, 0.793, 0.863, 0.797, and 0.931 for temperatures of 298K, 308K, 318K, 323K, and 328K, respectively, indicating adherence to the Temkin isotherm model. The adsorption capacity (AT) of activated tamarind kernel powder for Acid Red 1 was measured at 2.27 (l/g), 1.69 (l/g), 1.12 (l/g), 1.33 (l/g), and 2.21 (l/g) at the respective temperatures of 298K, 308K, 318K, 323K, and 328K. The results suggest that AT, which also represents the equilibrium binding constant corresponding to the maximum binding energy of the adsorbent, decreases as the temperature rises from 298K to 328K. The constant bT, which pertains to the heat of adsorption of activated tamarind kernel powder for Acid Red 1, is recorded as 552.4 (J/mg), 600.4 (J/mg), 668.8 (J/mg), 808.1 (J/mg), and 820.6 (J/mg) at 298K, 308K, 318K, 323K, and 328K, respectively. Additionally, Table 8 presents the Temkin adsorption isotherm models for Reactive Orange 20 within the same temperature range of 298K to 328K. The table indicates that the values are linear, with correlation coefficient (R2) values of 0.969, 0.865, 0.950, 0.910, and 0.928 at 298K, 308K, 318K, 323K, and 328K, respectively, further confirming compliance with the Temkin isotherm model. The adsorption capacity (AT) of activated tamarind kernel powder for Reactive Orange 20 was found to be 7.11 (l/g), 5.22 (l/g), 4.61 (l/g), 4.01 (l/g), and 2.37 (l/g) at the respective temperatures of 298K, 308K, 318K, 323K, and 328K.The findings indicate that AT, which represents the equilibrium binding constant associated with the maximum binding energy of the adsorbent, decreases as the temperature rises from 298K to 328K. The constant bT, which pertains to the heat of adsorption of activated tamarind kernel powder for Reactive Orange 20 at temperatures of 298K, 308K, 318K, 323K, and 328K, is recorded as 1138.0 (J/mg), 1167.7 (J/mg), 1158.1 (J/mg), 1292.3 (J/mg), and 1312.0 (J/mg) respectively. Table 8 illustrates the Temkin adsorption isotherm models for Reactive Blue 29 across the temperature range of 298K to 328K. From Table 8, it is evident that the values exhibit linearity, with correlation coefficient (R2) values of 0.992, 0.993, 0.960, 0.979, and 0.942 at 298K, 308K, 318K, 323K, and 328K respectively, indicating adherence to the Temkin isotherm model. The adsorption capacity (AT) of the activated tamarind kernel powder for Reactive Blue 29 is measured at 4.93 (l/g), 4.22 (l/g), 1.68 (l/g), 1.25 (l/g), and 1.47 (l/g) at 298K, 308K, 318K, 323K, and 328K respectively. The results further confirm that AT, which signifies the equilibrium binding constant corresponding to the maximum binding energy of the adsorbent, decreases as the temperature increases from 298K to 328K. The constant bT, which relates to the heat of adsorption of activated tamarind kernel powder for Reactive Blue 29 at 298K, 308K, 318K, 323K, and 328K, is noted as 683.5 (J/mg), 709.3 (J/mg), 945.6 (J/mg), 995.1 (J/mg), and 1173.0 (J/mg) respectively. Similar findings have been reported by Okoli *et al*. (2015) [13].

Table 8: Temkin Isotherm Constants for AR1, RB29 and RO20

Tempt (K)	Dye	A_T(J/mg)	b_T (l/g)	R2
	Acid Red 1			
298		2.24	552.4	0.921
308		1.69	600.4	0.913
318		1.12	668.8	0.953
323		1.33	808.1	0.971
328		2.21	820.6	0.987
Reactive Orange 20				
298		7.11	1138.0	0.969
308		5.22	1167.7	0.865
318		4.61	1158.1	0.950
323		4.01	1292.3	0.910
328		2.37	1312.0	0.928
Reactive Blue 29				
298		4.93	683.5	0.992
308		4.22	709.3	0.993
318		1.68	945.6	0.960
323		1.25	995.1	0.979
328		1.47	1173.0	0.942

Dubinin-Radushkevich (D-R) Isotherm

Table 9 illustrates the Dubinin Radushkevich adsorption isotherm models for Acid Red 1 across a temperature spectrum of 298K to 328K. It is evident that the values exhibit linearity, with correlation coefficient (R2) values recorded at 0.941, 0.932, 0.974, 0.965, and 0.933 for temperatures of 298K, 308K, 318K, 323K, and 328K respectively, indicating adherence to the Dubinin Radushkevich isotherm model. The saturation capacity constant (qD) for the activated tamarind kernel powder concerning Acid Red 1 was measured at 13.0 (mg/g), 13.2 (mg/g), 13.1 (mg/g), 13.0 (mg/g), and 12.76 (mg/g) at the respective temperatures of 298K, 308K, 318K, 323K, and 328K. The results suggest a decreasing trend in qD as the temperature rises from 298K to 328K. The constant BD, which pertains to the mean free energy of adsorption of Acid Red 1 on activated tamarind kernel powder, was found to be -1x10-5 (mol2/J2), -7x10-6 (mol2/J2), -4x10-6 (mol2/J2), -2x10-6 (mol2/J2), and -9x10-7 (mol2/J2) at 298K, 308K, 318K, 323K, and 328K respectively. Table 9 also presents the Dubinin Radushkevich adsorption isotherm models for Reactive Orange 20 within the same temperature range of 298K to 328K. The data indicates linearity, with correlation coefficient (R2) values of 0.923, 0.950, 0.963, 0.989, and 0.964 at 298K, 308K, 318K, 323K, and 328K respectively, further confirming the applicability of the Dubinin Radushkevich isotherm model. The saturation capacity constant (qD) for the activated tamarind kernel powder with respect to Reactive Orange 20 was recorded at 4.64 (mg/g), 5.53 (mg/g), 5.88 (mg/g), 6.50 (mg/g), and 6.51 (mg/g) at the respective temperatures of 298K, 308K, 318K, 323K, and 328K. The findings indicate an increasing trend in qD as the temperature escalates from 298K to 328K. The constant BD, which relates to the mean free energy of adsorption of Reactive Orange 20 on activated tamarind kernel powder, was determined to be -4x10-5 (mol2/J2), -3x10-5 (mol2/J2), -3x10-5 (mol2/J2), -2x10-5 (mol2/J2), and -1x10-5 (mol2/J2) at 298K, 308K, 318K, 323K, and 328K respectively.

Table 9 illustrates the Dubinin Radushkevich adsorption isotherm models for Reactive Blue 29 across a temperature spectrum of 298K to 328K. As indicated in Table 9, the values exhibit a linear trend, with correlation coefficients (R2) recorded at 0.923, 0.934, 0.789, 0.829, and 0.798 for temperatures of 298K, 308K, 318K, 323K, and 328K, respectively, suggesting adherence to the Dubinin Radushkevich isotherm model. The saturation capacity constant (qD) for the activated tamarind kernel powder in relation to Reactive Blue 29 was measured at 8.14 (mg/g), 8.63 (mg/g), 8.44 (mg/g), 8.73 (mg/g), and 8.87 (mg/g) at the respective temperatures of 298K, 308K, 318K, 323K, and 328K. The results indicate a rising trend in qD as the temperature escalates from 298K to 328K. The constant BD, which pertains to the mean free energy of adsorption of Reactive Blue 29 on activated tamarind kernel powder, was found to be -2x10-5 (mol2/J2), -2x10-5 (mol2/J2), -4x10-5 (mol2/J2), -3x10-5 (mol2/J2), and -2x10-5 (mol2/J2) at the temperatures of 298K, 308K, 318K, 323K, and 328K, respectively. The activation energy (EA) value provides insight into the nature of the adsorption process. Specifically, if the adsorption energy (EA) is below 8kJ/mol, the process is classified as physical (physisorption); conversely, if it falls between 8 and 16kJ/mol, it is categorized as chemical adsorption (chemisorption). The EA values determined for Acid Red 1 dye adsorption on activated tamarind kernel powder were 0.22kJ/mol, 0.27kJ/mol, 0.35kJ/mol, 0.50kJ/mol, and 0.74kJ/mol at system temperatures of 298K, 308K, 318K, 323K, and 328K, respectively. For Reactive Orange 20 dye adsorption on activated tamarind kernel powder, the EA values were 0.11kJ/mol, 0.13kJ/mol, 0.13kJ/mol, 0.16kJ/mol, and 0.22kJ/mol at system temperatures of 298K, 308K, 318K, 323K, and 328K, respectively. The EA values for Reactive Blue 29 dye adsorption on activated tamarind kernel powder were recorded at 0.16kJ/mol, 0.16kJ/mol, 0.35kJ/mol, 0.41kJ/mol, and 0.50 kJ/mol at system temperatures of 298K, 308K, 318K, 323K, and 328K, respectively. The mean free energy values obtained are less than 8kJ/mol, indicating that Acid Red 1 dye, Reactive Orange 20 and Reactive Blue 29 adsorption on activated tamarind kernel powder is a physical process or physisorption. Similar results are reported by (Obruche *et al*., 2025) [12].

Table 9: Dubinin Radushkevich Isotherm Constant for AR1, RB29 and RO20

Tempt (K)	Dye	B_D (mol^2/J^2)	q_D (mg/g)	R2
	Acid Red 1			
298		$-1x10^{-5}$	13.0	0.941
308		$-7x10^{-6}$	13.2	0.932
318		$-4x10^{-6}$	13.1	0.974
323		$-2x10^{-6}$	13.0	0.965
328		$-9x10^{-7}$	12.76	0.933
Reactive Orange 20				
298		$-4x10^{-5}$	4.64	0.923
308		$-3x10^{-5}$	5.53	0.950
318		$-3x10^{-5}$	5.88	0.963
323		$-2x10^{-5}$	6.50	0.989
328		$-1x10^{-5}$	6.51	0.964
Reactive Blue 29				
298		$-2x10^{-5}$	8.14	0.923
308		$-2x10^{-5}$	8.63	0.934
318		$-4x10^{-6}$	8.44	0.789
323		$-3x10^{-6}$	8.73	0.829
328		$-2x10^{-6}$	8.87	0.798

Adsorption Kinetics

In this research, two distinct models were employed, namely the pseudo-first-order and the pseudo-second-order models. The aforementioned pseudo-first-order and pseudo-second-order kinetic models were utilized to evaluate the equilibrium data, aiming to explore the adsorption mechanism and identify the potential rate-controlling step of the adsorption process. Nevertheless, to determine the optimal conditions for executing full-scale batch dye removal processes, it is essential to have information regarding the kinetics of dye adsorption. A kinetic analysis was conducted at various time intervals, maintaining a constant initial dye concentration and adsorbent dosage. The pseudo-first-order and pseudo-second-order kinetics modeling for the adsorption of Acid Red 1, Reactive Orange 20, and Reactive Blue 29 dyes onto TKP is illustrated in Table 10 and Table 11, respectively. The experimental adsorption capacities for Acid Red 1, Reactive Orange 20, and Reactive Blue 29 were found to be 3.95 mg/L, 1.50 mg/L, and 2.58 mg/L, respectively. The adsorption capacities calculated using the pseudo-first-order model were reported in Table 10 as 2.41 mg/L, 3.53 mg/L, and 2.56 mg/L, respectively, while the capacities derived from

the pseudo-second-order model are presented in Table 11 as 4.29 mg/L, 2.44 mg/L, and 2.95 mg/L, respectively. The calculated adsorption capacities for all dyes using the pseudo-second-order model were observed to be very close to their corresponding experimentally determined adsorption capacities, as indicated in Table 11. In contrast, a significant discrepancy was noted when comparing the adsorption capacities obtained from the pseudo-first-order kinetics with the experimentally determined values. The correlation coefficients, R2, derived from the pseudo-first order adsorption model for the dyes Acid Red 1, Reactive Orange 20, and Reactive Blue 29 were recorded as 0.074, 0.347, and 0.107, respectively. In contrast, the R2 values for the pseudo-second order kinetics were found to be 0.999, 0.847, and 0.993 for Acid Red 1, Reactive Orange 20, and Reactive Blue 29, respectively. The results indicate that the R2 values from the pseudo-second order kinetic plot surpass those from the pseudo-first order adsorption kinetic plot. Consequently, the correlation coefficient values and the calculated adsorption capacities for all the dyes do not conform to the pseudo-first order kinetic model, implying that the adsorption of Acid Red 1, Reactive Orange 20, and Reactive Blue 29 onto activated tamarind kernel powder is influenced by the initial concentration. Therefore, the pseudo-second order adsorption model is more appropriate for characterizing the adsorption kinetics of Acid Red 1, Reactive Orange 20, and Reactive Blue 29 onto ATKP, based on the premise that adsorption may represent the rate-limiting step (Gupta and Rastogi, 2007). The kinetic data obtained holds considerable practical significance for technological applications, as kinetic modeling effectively substitutes for time-intensive and resource-consuming experiments required for the design of process equipment (Oladunni *et al*., 2012) [15].

Table 10: Pseudo-First order Kinetic Constant for AR1, RO20 and RB29

Dye	$k_1(min^{-1})$	q_e (mg/g) (calculated)	R2
Acid Red 1	0.005	2.41	0.074
Reactive Orange 20	0.0092	3.43	0.347
Reactive Blue 29	0.0069	2.56	0.107

Table 11: Pseudo-Second order Kinetic Constant for AR1, RO20 and RB29

Dye	k_2 (g/mg.min)	q_e (mg/g) (calculated)	R2
Acid Red 1	0.03	4.29	0.999
Reactive Orange 20	0.009	2.44	0.847
Reactive Blue 29	0.002	2.95	0.993

Conclusion

In this study, the characterization analysis performed on the activated carbon revealed that all parameters, including bulk density, pH, ash content, and dry matter, fell within an acceptable range. The FTIR analysis conducted on the raw activated tamarind kernel powder demonstrated the presence of various functional groups, such as hydroxyl, alkanes, alkenes, alkynes, carboxyl, phenols, phosphates, carbonyl, and both primary and secondary amines, which serve as significant adsorption sites on the surface of the adsorbent. Furthermore, the FTIR analysis of the dye-adsorbed activated tamarind kernel powder showed the emergence of certain functional groups that were absent in the FTIR spectrum of the raw ATKP. The investigation into the effects of various parameters, including pH, adsorbent dosage, initial dye concentration, contact time, and temperature, indicated that the adsorption of Acid Red 1, Reactive Orange 20, and Reactive Blue 29 from simulated dye-based wastewater utilizing activated tamarind kernel powder is influenced by these factors. Among the four equilibrium isotherms evaluated in this study, the data obtained best aligned with the isotherm models in the following order: Langmuir > Temkin > Dubinin-Radushkevich > Freundlich. Additionally, from the adsorption kinetic models assessed, the Pseudo-Second order kinetic model provided the most accurate representation of the adsorption kinetics observed. This research clearly demonstrates that activated tamarind kernel powder possesses the ability to effectively remove Acid Red 1, Reactive Orange 20, and Reactive Blue 29.

References

1. Abeokuta OJ, Uriri SA, Obruche EK, Okurame O. Hydrochemical Assessment of Borehole Water Quality in Eku, Delta State, Nigeria. Journal of Science, Technology and Environmental Studies,2025:1(2):17-25
2. Al-Degs YS, MI El-Barghouthi, MA Khraisheh, MN Ahmad, SJ Allen. ―Effect of Surface Area, Micropores, Secondary Micropores and Mesopores Volumes of Activated Carbons on Reactive Dyes Adsorption from Solution, ‖ Separation Science and Technology,2004:39(1):97-111
3. Andre LC, Alexandro MM, Eurica MN, Marcos HK, Marcos RG, Alessandro CN, *et al*. NaOH Activated Carbon of High Surface Area Produced from Coconut Shell: Kinetics and Equilibrium Studies from the Methylene Blue Adsorption. Chemical Engineering Journal,2011:174:117-125.
4. Arita IH, Castano VM, Wilkinson DS. Synthesis and Processing of Hydroxyapatite Ceramic Tapes with Controlled Porosity. Journal of Materials Science,1995:6(1):19-23.
5. ASTM Committee on Standards, American Society for Testing and Materials: Standard for Method for Moisture in Activated Carbon. Philadelphia, PA: ASTM Committee on Standards, 2003.
6. Bapat P, Nandy SK, Wangikar P, Venkatesh KV. Quantification of metabolically active biomass using Methylene Blue dye Reduction Test (MBRT): Measurement of CFU in about 200 s. Journal ofMicrobiological Methods,2006:65:107–116.
7. Ekpo Ekokodu Rose, Erienu Obruche Kennedy, Abiye Clement. Marcus Spatial and Temporal Variations in the Concentrations of Polycyclic Aromatic Hydrocarbon, in Ambient Air from Three Different Locations in River State, Nigeria. International Journal of New Chemistry,2025:12(4):567-580
8. El-Hendawy AA, Alexander RJ, Andrews GF. Effect of Activation Schemes on Porous Surface and Thermal Properties of Activated Carbons Prepared from Cotton Stalk, Journal of Analytical Applicationin Pyrolysis,2008:82:272-278.
9. Erienu Obruche Kennedy, Itodo Adams, Wuana Raymond, Sesugh Ande. Polycyclic Aromatic Hydrocarbons in Harvested Rainwater in Warri and Agbarho, Nigeria. Bulletin of chemical society of Ethiopia,2022:36(4):27-35.

10. Festus-Amadi IR, Erhabor OD, Ogwuche Christiana E, Obruche EK. Characterization of Contaminated Sediments Containing Polycyclic Hydrocarbons from Three Rivers in the Niger Delta Region of Nigeria. Chemistry Research Journal,2021:6(3):1-12
11. Itodo AU, Wuana RA, Erhabor OD, Obruche EK, Agbendeh ZM. Evaluating the Effects of Roofing Materials on Physicochemical Properties of Harvested Rainwater in Warri, Delta State, Nigeria. Chemical Society of Nigeria Journal, Kano,2021:12(1):234-245
12. Obruche EK, Emakunu SO, Ugochukwau GC. Rainwater Harvesting: Microbial and Chemical Water Quality Assessment in Warri District. Mosogar Journal of Science Education,2025:10(1):36-45
13. Okoli CA, Onukwuli CD, Okey-Onyesolu CE, Okoye CC. Adsorptive Removal of Dyes from Synthetic Waste water using Activated Carbon from Tamarind Seed. European Scientific Journal,2015:11(18):190-221. Okiemmen, F., Okiemen, C., and Wuana, A. (2008). Preparation and Characterization of Activated Carbon from Rice Husk.Journal of Chemical Society of Nigeria, 32, 126-136
14. Obruche Ek, Erhabor OD, Itodo AU, Itopa ST. Spectrophotometric determination of iron in some commercial iron containinig tablets/capsule. International journal of advanced trends in computer applications,2019:1(1):231-235
15. Oladunni N, Agbaji EB, Idris SO. Removal of Pb2+ and Ni2+ from aqueous solutions by adsorption onto activated locust bean (Parkia Biglobosa) husk. Archives of Applied Science Research,2012:4(5):2161-2173.
16. Obruche EK, Ogwuche CE, Erhabor OD, Mkurzurum C. Evaluation of the inhibitive effect of African Marigold (*Tagetes erectal L*.) Flower Extracts on the Corrosion of Aluminium in Hydrochloric Acid. International Journal of Advances in Scientific Research and Engineering,2018:4(12):167-177
17. Oladoja NA, Aboluwoye, Olademeji. Kinetics and Isotherm Studies on Methylene blue Adsorption onto Ground palm Kernel Coat. Turkish Journal of engineering and Environmental Science,2008:32:303-312.
18. Obruche EK, Ogwuche CE, Erhabor OD, Mkurzurum C. Investigating Corrosion Inhibition Effects of *Tagetes Erecta L*. Leaf Extrac on Aluminium in Acidic Medium. Global Scientific Journals,2019:7(1):1-17
19. Ogwuche CE, Obruche EK. Physio-chemical analysis of palm oils (*elaeis guineensis*) obtained from major markets in agbarho, unenurhie, opete, ughelli and evwreni town, Delta state, Nigeria. International journal of trend in scientific research and development,2020:4(2):56-60
20. Olugbenga SB, Oladipo MA, Misbaudeen AH, Olalekan AMP. Kinetic and Equilibrium Studies of Methylene Blue Removal from Aqueous Solution by Adsorption on Treated Sawdust. Macedonian Journal of Chemistry and Chemical Engineering,2010:29(1):77–85.
21. RE Ekpo, AC Marcus, EK Obruche. Spartial and Temporal Variations in the Concentration of Particulate Matter in Ambient Air from three Different Locations in River State, Nigeria. International Journal of Scientific Research in Chemical Science,2023:10(4):32-38
22. Umudi EQ, Obruche EK, Sani MI, Onwugbuta GC, Aghemwenhio IS, Ikechukwu SC, *et al*. Evaluation of Polycyclic Aromatic Hydrocarbons (PAHs) Contents of Fishes, Waters and Sediments of Rivers Niger: Human Health Risk Assessment. Journal of Basics and Applied Sciences Research,2025:3(5):187-199. https://dx.doi.org/10.4314/jobasr.v3i5.20
23. Ucello-Berrata G, Nazzi S, Balzano F, Dicolo G, Zambito Y, Zaino C, *et al*. Enhanced Affinity of Ketotifen Towards Tamarind Seed Polysaccharide in Comparison with Hydroxyethylcellulose and Hyaluronic Acid: A Nuclear Magnet Resonance Investigation. Journal of Bioorganic and Medicinal Chemistry,2008:16:7371- 7376.
24. Umudi Ese Queen, Ese Ekanem, Sani Mamman Ibrahim, Onwugbuta Godpower Chukwuemeka, Suleiman Abdulmajid, Magashi Luper, Udo Idongesit, *et al*. Degradation Efficiencies of the Total Petroleum Hydrocarbons (TPHs) in the Soil Amended with Palm Bunch Ash and Tween 80 in Ibenomo L.G.A, Akwa Ibom State. International Journal of Chemistry and Chemical Processes,2025:11(5):1-20 10.56201/ijccp.vol.11.no5.2025.pg1.21
25. Umanah FI, Oyibo RU, Rita CN, Bashir MA, Ibebuike UO, Obruche EK. Self-Concept, Self-Efficacy and Parental Involvement as Predictors of Academic Achievement of Junior Secondary School Students in Delta South Senatorial District. Journal of Education Research and Library Practice,2025:9(8):51-65
26. Umudi Ese Queen, Odontimi Nimighaye, Sani Mamman Ibrahim, Chidi Henry, Onwugbuta Godpower Chukwuemeka, Odejobi BabajideMichael, *et al*. Assessment of the Seasonal Variations in Heavy Metals Concentration in the Ughelli Central Market River, Delta State, Nigeria. International Journal of Applied Science and Mathematical Theory,2025:11(6):78-88. https//doi.org/10.56201/ijasmt.vol.11.no6. 2025.pg78.88
27. Ugochukwu Gladys Chioma, Ataine Theresa Ifeyinwa, Erienu Kennedy Obruche. Determination of the Physicochemical Properties of Soil Amended with Cassava Mill Effluent in Mosogar Area of Delta State. Mosogar Journal of Science Education,2025:10(1):81-89
28. Umudi Ese Queen, Ese Ekanem, Idongesit O Ekpenyong, Sani Mamman Ibrahim, Onwugbuta Godpower Chukwuemeka, Suleiman Abdulmajid, *et al*. Seasonal Assessment of Heavy Metals Concentrations in Sediment of the Sapele River, Nigeria Journal of Science Innovation & Technology Research,2025:9(9):124–139